# Visual areas involved in the perception of human movement from dynamic form analysis

Lars Michels,[1,CA] Markus Lappe[1] and Lucia Maria Vaina[2,3]

[1]Psychologisches Institut II, Westfälische Wilhelms-Universität, Münster, Germany; [2]Brain and Vision Research Laboratory and Neurovisual Clinic, Boston University; [3]Harvard Medical School, Department of Neurology 3, Massachusetts, USA

[CA]Corresponding Author: michelsl@psy.uni-muenster.de

Received 26 April 2005; accepted 27 April 2005

The perception of biological motion combines the analysis of form and motion. However, patient observations by Vaina *et al.* and psychophysical experiments by Beintema and Lappe showed that humans could perceive human movements (a walker) without local image motion information. Here, we examine the specificity of brain regions responsive to a biological motion stimulus without local image motion, using functional magnetic resonance imaging. We used the stimulus from Beintema and Lappe and compared the brain activity with a point-light display that does contain local motion information and was often used in previous studies. Recent imaging studies have identified areas sensitive to biological motion in both the motion-processing and the form-processing pathways of the visual system. We find a similar neuronal network engaged in biological motion perception, but more strongly manifested in form-processing than in motion-processing areas, namely, fusiform-/occipital face area and extrastriate body area. *NeuroReport* 16:1037–1041 © 2005 Lippincott Williams & Wilkins.

**Key words**: Biological motion; Functional magnetic resonance imaging; Local motion; Ventral pathway

## INTRODUCTION

One of the most compelling examples of the visual system's ability to recover object information from sparse input is provided by the phenomenon known as biological motion (BM). People can recognize actions performed by others, even when these movements are portrayed by a stimulus that consists of just light points attached to the major joints of the body [1]. It is often assumed that the recognition of BM is a highly specialized part of motion analysis that leads to a perception mechanism called form-from-motion. Recent studies of BM showed the involvement of brain areas that underlie the perception of BM [2–7]. The brain activation was located in the posterior superior temporal sulcus (pSTS). The STS receives projections from both pathways of the visual system: the dorsal pathway that processes primarily motion information and the ventral pathway that processes mainly color and form information. Reciprocal connections within the dorsal pathway connect pSTS with the motion responsive areas medio temporal (MT) and medio superior temporal (MST). The input from the ventral pathway into the STS comes from form responsive areas V3 and V4. Therefore, STS activation can result from analysis of either form or motion signals in the visual input. Similarly, BM recognition could be derived from form or motion cues. Vaina *et al.* [8] described a patient (A.F.) with bilateral motion impairment. A.F. could not solve basic motion tasks but was able to perceive BM. Furthermore, McLeod *et al.* [9] studied a patient (L.M.) with bilateral lesions along the dorsal pathway (including MT), who was almost 'motion-blind' but was able to recognize human actions in point-light displays. Schenk and Zihl [10,11] described two patients with normal sensitivity to coherent motion, but with strong inability to perceive BM figures portrayed against a background of a static noise pattern. These studies indicate that BM perception differs fundamentally from other kinds of motion perception. Specifically, form information may be used in BM perception by integrating the static form information of individual frames of the stimulus sequence over time [12,13]. In this view, the visual system would first analyze the shape of the human figure from form cues such as the distribution of light-point on the body. Subsequently, the motion of the body is derived from an analysis of the transformation of the shape over time. This procedure eventually captures both form and motion aspects of BM but the motion is derived from form analysis rather than from low-level motion perception. A computational model using this approach quantitatively captures many of the properties of BM perception [13]. Imaging studies support this idea, showing that BM selectivity is not just restricted to pSTS but involves also two areas of the ventral stream: the occipital face area (OFA) and the fusiform face area (FFA), which are part of the fusiform gyrus [2–7,14]. Whether the extrastriate body area (EBA), which responds to bodies or body parts, is selectively activated by BM, is not fully clear yet [2,14].

Beintema and Lappe [12] have introduced a variant of the classical BM stimulus to investigate the role of form information in the perception of BM. This stimulus provides a way to study the perception of BM when it is not supported by low-level motion signals. With this stimulus, we investigate the neuronal network engaged in the perception for BM stimuli with and without local motion

signals. Our hypothesis is that the brain activation to a BM stimulus that contains primarily form information (and no local image motion) is stronger in form-processing than in motion-processing areas. We would regard this as evidence for a route to BM perception that bypasses the motion pathway.

## MATERIALS AND METHODS

***Stimuli:*** In Johansson's classic point-light walker (CW stimulus, Fig. 3a) one light point is placed at each of the major joints of the body. We use a computer algorithm, which simulates a walker that walks in place on a treadmill and consists of 10 dots located on the ankles, knees, the hip, wrists, elbows and the shoulder [15]. In the sequential position walker (SW, Figs. 1 and 3c) stimulus, introduced by Beintema and Lappe [12], eight light points appear at random locations on the imaginary lines connecting the major joints of the walker's body. Each point is shown for just one frame of the stimulus animation (54 ms). In the next frame, it is relocated to another random position between the joints. Thus, an individual point does not provide a consistent motion signal because it cannot be tracked over frames. The frequent relocation of the dots instead provides increased form information as the limbs are traced over time. Observers recognize this new stimulus spontaneously as a walking human figure [12]. The starting phase in the sequence of each step cycle for both walkers was varied randomly from trial to trial. For each walker type, we also included a static condition (CS and SS, respectively) in which the walker was presented in a single static posture. For the CS stimulus, one randomly chosen static frame of the CW was shown throughout the trial (Fig. 3b). For the SS stimulus, the walker remained in a single randomly chosen posture throughout the trial, but the dots were relocated in each frame to new positions between the limbs (Fig. 3d). Together, we therefore presented four conditions (CW, CS, SW and SS). All stimuli subtended 5° by 11° of visual angle and were composed of luminous (red/green) square dots (0.2°) presented on a black screen (visual field 40° × 25°, frame rate of 60 Hz).

***Experimental design:*** The functional magnetic resonance imaging (fMRI) experiment was done in an on–off block design. Study participants performed two discrimination tasks while fixating a green fixation dot (0.2°) in the center of the screen.

Each on-period contained one of the four experimental conditions. Participants saw blocks of 60 s duration, in which half the trials presented the specific walker (CW, CS, SW or SS) and the other half presented phase-scrambled versions of the same walker type. In the phase-scrambled stimuli, the starting phase of each joint angle was randomly chosen. The resulting stimuli contain local motion of the limb segments similar to a normal walker but in a configuration that is inconsistent with the human body structure. Previous studies using this scrambled stimulus pointed out that the outline depicting a human figure was not visible in this condition [2,3,16]. Participants had to respond about whether the stimulus depicted as a human figure. The blocks were presented in a pseudorandomized order and were repeated three times during scanning. The duration of a single trial was 1.6 s, with 1 s stimulus presentation (=0.625 of a step cycle). In half the trials, stimuli were oriented leftward, and in the other half, rightward.

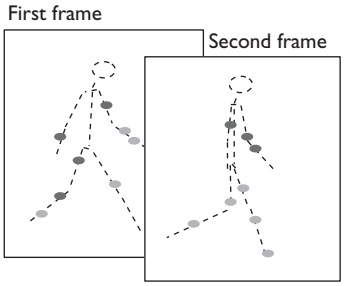


**Fig. 1.** Example of the new biological motion stimulus [sequential position walker (SW)] in two consecutive frames. Dots lived only one frame after which they were relocated to a random position between the joints. The dashed lines of the body and the head were not shown in the experiment.

In the off-period (baseline, 30 s/block), participants saw eight stationary dots at random positions within an area of the same width and height as the walker stimulus. Four of the dots changed luminance to an increased or decreased level at a random time of 0.4–0.7 s after trial onset. The direction of the luminance change was determined randomly. The task was to maintain attention and detect a luminance change in an array of the dots. After 1 s stimulus presentation, the screen turned dark for 0.6 s except for the fixation dot. Participants responded about whether the four dots became brighter or darker on a keypad connected to the computer.

***Study participants:*** Four neurologically healthy males (mean age 22 years) gave informed consent for the experimental protocol approved by the MGH Human Subjects Committee. The participants were naive with respect to the hypothesis of the study.

***Magnetic resonance scanning:*** A 1.5 T GE Horizon Echo-Speed was used, retrofitted for echoplanar imaging. A conventional volume was acquired by using 22 6-mm-thick contiguous oblique slices (3.13 × 3.13 mm in plane) parallel to a line drawn between the anterior commissure–posterior commissure, sufficient to cover the whole brain. A flow series was obtained in the oblique planes selected for functional scanning to detect major blood vessels, followed by a T1-weighted sagittal localizer series [repetition time (TR)=6 s, field of vision (FOV)=20 $cm^2$]. Functional images acquired using the blood oxygenation-level-dependent (BOLD) technique were obtained by applying an asymmetric spin echo pulse sequence (22 axial slices, TR/TE=2500/30 ms, flip angle=90°). A high-resolution three-dimensional structural scan for each participant was also acquired during the same session (114 slice sagittal partitions, TR/TE=2500/4 ms, FOV=20 $cm^2$).

***Data analysis:*** Echoplanar images were post-processed with MEDX 3.3 software (Sensor Systems, Sterling, Virginia, USA). The first four scans of each run were excluded from analysis to avoid differences in T1 saturation. The steps for

**Table I.** Activations referring to maxima z-values (>25 activated neighboring voxels; $p<0.05$, corrected) in regions of interest.

| Area | RH | | | CW | CS | SW | SS | LH | | | CW | CS | SW | SS |
|---|---|---|---|---|---|---|---|---|---|---|---|---|---|---|
| | *x* | *y* | *z* | Maximum z-score | | | | *x* | *y* | *Z* | Maximum z-score | | | |
| EBA | 40 | −69 | 4 | 15.7 | 6.8 | 10.9 | 12.5 | −41 | −68 | 3 | 14.8 | 5.1 | 10.9 | 10.1 |
| MT | 42 | −62 | 2 | 13 | 5.8[2] | 13.9 | 12.8 | −42 | −64 | 1 | 14.4 | 3.6[1] | 14.9 | 12.1 |
| KO | 29 | −86 | 1 | 5.4 | 5.4[3] | 10.1 | 11.7 | −27 | −84 | 2 | 4.6 | 4.2[2] | 7.5 | 7.3 |
| FFA | 40 | −41 | −14 | 8.3 | 5.1 | 9.9 | 11.4 | −34 | −40 | −14 | 9.1 | 5.7[2] | 7.4 | 7.6 |
| pSTS | 52 | −43 | 12 | 5.8 | 3.5[2] | 5.5[3] | 5.4 | −44 | −50 | 11 | | | | 3.8[1] |
| QuP | 32 | −68 | −19 | 6.9[2] | 3.8 | 8.7[2] | 10 | −31 | −72 | −18 | 8.1[2] | 5.1 | 10.1[2] | 8.7 |
| IFG | 42 | 32 | 12 | 5.1 | 9.3 | 7.8[3] | 11.3 | −41 | 24 | 10 | 4.1[3] | 5.2 | 5.5 | 6.2 |
| sPrG | 32 | 5 | 52 | 4.9 | 8.1 | 7.2 | 6.9 | −36 | 3 | 55 | 4.1 | 6.3[3] | 6.5 | 8.1 |
| LG | 16 | −84 | 0 | 8.4 | 4.7 | 8.7 | 10.4 | −12 | −86 | 0 | 8.1 | 6.3 | 10.3 | 8.7 |

The superscript digits indicate that activation could not be found in all participants; for example, a superscript digit of 1 indicates activation was found only in one participant.

head motion correction, spatial and temporal smoothing of the time series are explained in detail by Vaina *et al.* [4,17]. For each participant, the combined *z* maps (of each condition of the on-period) were set to a voxel activation threshold of $p<0.05$ ($z=3$) and were superimposed onto the participant's high-resolution MRI in Talairach space [18]. As done by Vaina *et al.* the *z* maps were taken from the subtraction of the averaged signal of the off-period from the averaged signal of the on-period (the averaged signal of all BM and scrambled events within a block) [4,17]. For the group analysis, the Talairach registered *z*-score map images of all runs and participants were summed and then divided by the square root of the total number of scans, providing a group z-score map (corrected for multiple comparisons) for each condition.

The cluster threshold for later analysis was set to a minimum of >25 activated neighboring voxels. We examined the mean percent signal change of the BOLD signal in specific regions of interest (ROIs). The dimension of an ROI [MT, pSTS, EBA, FFA/OFA, lingual gyrus (LG), inferior frontal gyrus (IFG), posterior portion of the quadrangular lobule (QuP) and kinetic occipital (KO)] was defined as follows. For each participant, the location of an ROI was identified on the basis of anatomical landmarks. Then, a mean (fixed) Talairach coordinate for each ROI was determined across participants. The depth and size of an ROI varied between areas. The spatial extent was within accepted and published ranges for each ROI. Because the activations to BM in FFA and OFA were very similar [2], we averaged the signals of both ROIs and report a combined activity for FFA/OFA. We performed an MT localizer test for each participant to differentiate MT from the anatomically close area EBA. Here, participants saw blocks (duration 60 s, three repetitions) of contracting and expanding dots while fixating a central fixation dot. On the basis of the activation map of the localizer test, we adjusted the size of the anatomically predefined ROI for MT.

***Prescan:*** For later analysis of the fMRI signal, it was necessary that the off-period and the on-period had the same difficulty in decision-making. Therefore, participants were trained before scanning for both discrimination tasks. The collected data of both tasks were analyzed to compare the percent correct ratio. The training phase was repeated until the participants reached a stable performance level of at least 80% correct for both tasks. This took on average 245 trials per condition and participant. After the subsequent scanning session, a two-way repeated-measures ANOVA with the factors condition and time (before and during scanning) revealed no significant difference in the performance among the four conditions of the on-period [$F(31,1)=2.5$, $p=0.13$] or the off-period and no training effect comparing the performance before and during scanning [$F(28,3)=0.48$, $p=0.7$ for the on-period].

## RESULTS

We examined the functional brain activity among four contrasts (CW, CS, SW and SS vs. baseline). The whole-brain analysis revealed significant effects of stimulus type in several regions (Table 1). In Fig. 2, the group mean percent magnetic resonance signal change (with SEM) from the baseline for the ROI templates is plotted. Part of the averaged activity maps for the group is shown in Fig. 3, with the foci on some of the ROIs.

Activation was obtained in FFA/OFA in all conditions bilaterally compared with the baseline. A repeated-measures ANOVA with the factor condition and ROI revealed a significant effect [$F(31,3)=4.6$, $p<0.03$]. Further, Fisher's post-hoc tests showed that SW and SS were significantly higher activated than CW (SW to CW: $p<0.05$; SS to CW: $p<0.04$) and CS (SW to CS: $p<0.02$; SS to CS: $p<0.02$). No significant differences were obtained comparing CW with CS ($p<0.56$) and SW with SS ($p<0.97$). Similar to earlier studies of BM [2–7], activation occurred in the right pSTS (bilateral in one participant in the SS), which was significantly higher for CW, SW and SS than for CS (see Fig. 2). In all conditions tested, comparison in the ROI of EBA revealed significantly stronger activation for SW and SS than for CW and CS (see Fig. 2). The activation in frontal regions, especially in the left IFG, was significantly higher for CS than for CW ($p<0.02$, post-hoc test). Also, weak but significant activation was found in the premotor cortex in the inferior and the superior precentral gyri bilaterally for all four experimental conditions. We observed robust activation in the cerebellar lobule VI (QuP) [4,19].

Activation in motion-sensitive areas of the dorsal pathway (MT and KO) was strong but showed no significant differences between CW, SW and SS (repeated-measures ANOVA). Comparing SW with CW, the effect in the left KO was marginally significant ($p=0.058$). The CS condition gave

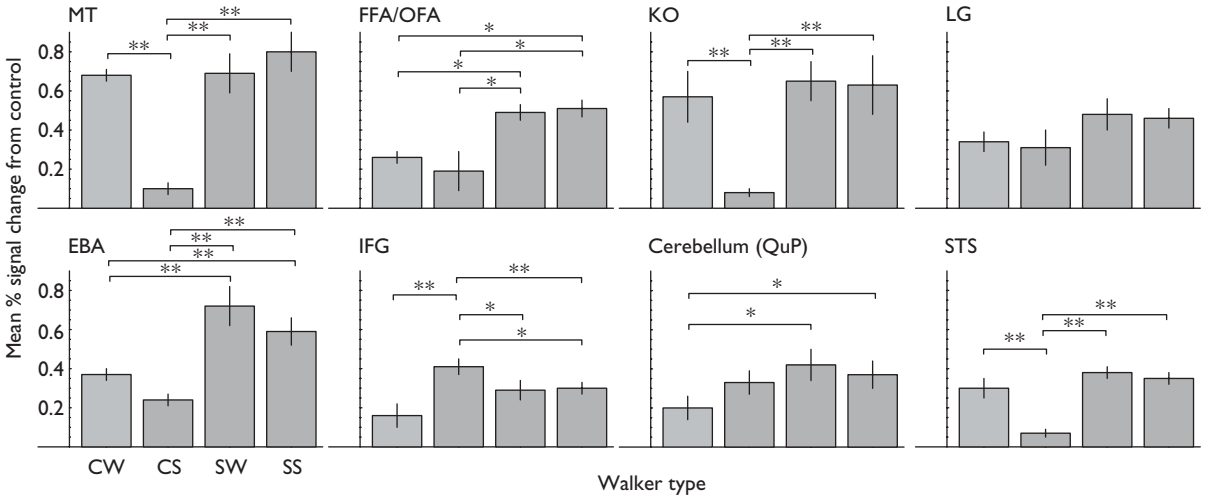


**Fig. 2.** Mean percent signal change for the group (with SEM) for the specific biological motion conditions [classical walker (CW), classical static walker (CS), sequential position walker (SW) and sequential static walker (SS)] versus baseline in regions of interest. The results were averaged across both hemispheres [superior temporal sulcus (STS) only activation in the right hemisphere]. *highlights significant differences at $p < 0.05$, **at $p < 0.01$.

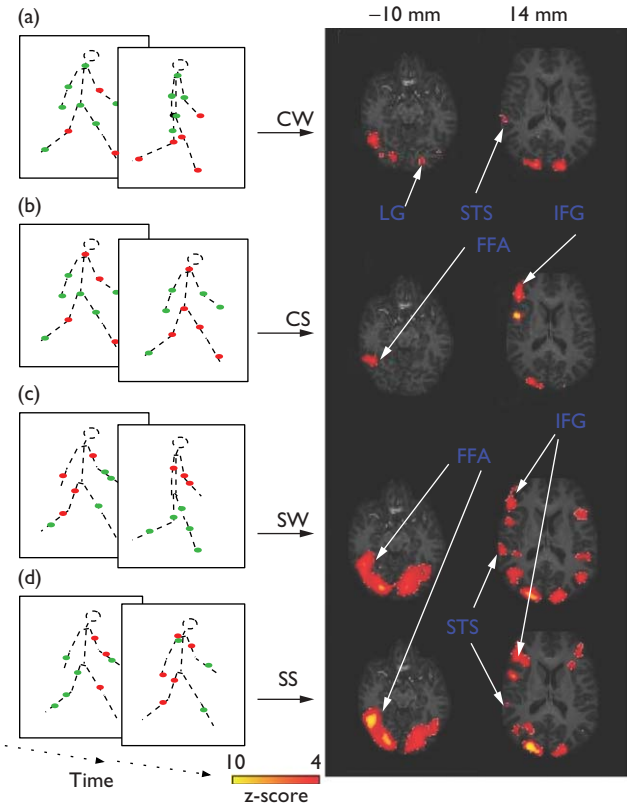


**Fig. 3.** Group activation map for each contrast [classical walker (CW), classical static walker (CS), sequential position walker (SW) and sequential static walker (SS) vs. baseline] in two different axial slices. (**a**)–(**d**) show the stimulus properties in two consecutive frames. Activation was strong in areas of the ventral stream for the new stimulus [e.g. fusiform face area (FFA)]. (**c**) and (**d**). Right in the images corresponds to left in the participants. Color scale represents z-score.

significantly lower activation. Further post-hoc analysis showed that this was true for the right and the left hemisphere (all $p < 0.05$).

## DISCUSSION AND CONCLUSION

In this study, we used a new BM stimulus (sequential position walker, SW) to examine the role of form information in the perception of BM. Like most previous neuroimaging studies of BM, we found activation in the pSTS [2–7]. We provide three new findings for pSTS. First, the (right) pSTS responds significant lower to stimuli without motion information (CS), probably because of the missing dynamic signal. Second, STS activation was similar to BM stimuli that contain local motion (CW) and to stimuli that contain no local motion information (SW, SS). Third, STS responds similarly to BM stimuli with different amounts of form information (comparing SW and SS with CW). This suggests that STS, on the one hand, discriminates between BM and nonbiological motion, but is not dependent on local motion signals in the BM stimulus.

A major conclusion of our study is that form-processing areas are differentially activated by different BM stimuli. We found increased activation in the fusiform gyrus (FFA/OFA) and EBA for stimuli possessing primarily form information (SS and SW) compared with stimuli with less form information (CW and CS). This is consistent with earlier studies showing form-based activation of the ventral pathway in the perception of BM [2,4,5,7,14,20]. For example, when fMRI responses to video and point-light displays of moving humans were compared, strong activations in the ventral temporal cortex occurred for human videos and weak activations occurred for point-light animations of BM, especially in the lateral fusiform gyrus [7]. The authors suggested that form, but not motion, contributes to the activation in the ventral cortex.

We found that in EBA, which is also activated by BM, activation was dependent on the type of BM stimulus [2,14]. Activation was significantly stronger for stimuli that possess strong form cues (SW, SS) than for classical BM stimuli (CW, CS). As mentioned earlier, the SW and SS stimuli convey stronger form information by tracing the outline of the figure. We suggest that this additional form information could be responsible for the higher activation in EBA than in CW, where no contours were visible. Furthermore, EBA

responses were similar to moving and static stimuli of each respective stimulus type (CW similar to CS, SW similar to SS). This is consistent with previous work showing that EBA is activated by both moving and static human figures [2,14].

Unlike ventral stream areas, the CW, SW and SS stimulus similarly activated motion-sensitive areas KO and MT. Similar activation by CW and SW may occur because both stimuli present a moving walker. The motion of the limbs may drive MT and KO responses even if local motion signals are missing as in the SW case. However, this does not explain the activation of the SS stimulus. Activation by the SS stimulus (and also possibly the SW stimulus) could result from the flickering of the dots, which may induce illusionary contours and possibly some apparent motion along the limbs. Dorsal stream areas are known to respond to flicker revealed by fMRI [21,22]. However, responses to flicker are usually smaller than responses to real motion [23]. This is also true for the ventral pathway, for both apparent and real motion [24].

We also obtained activation in frontal regions, here in the IFG and the superior precentral sulci (part of the premotor cortex). Higher activation of the (left) IFG could be due to the comparison of possible human figures with impossible ones [25]. This specificity in the IFG was shown in another brain imaging study [25]. Although the performance level for the four conditions was very similar, it seems plausible that stimuli containing intact motion information (CW) or strong form information (SW, SS) are much more vivid than CS. Possibly, participants were simply faster in decision-making, which could result in less IFG activation. Indeed, a two-way ANOVA with the factor condition and ROI showed an effect of response time ($p < 0.03$, post-hoc test). The responsiveness to BM in the premotor cortex could result from the involvement of the premotor cortex in action observation [26]. Premotor cortex activation by BM was previously described by Saygin *et al.* [6]. The authors concluded that the observer's motor system is recruited to fill in the simplified BM displays and that the motion information in body actions can drive frontal areas. In our data, premotor cortex activation in the static CS and SS conditions also occurred, although this activation was less extensive compared with the moving conditions. This difference could possibly explain why Saygin *et al.* found activation when they compared BM with static point-light figures.

In summary, our study revealed that the activations to BM in areas of the ventral stream (FFA/OFA and EBA) were dependent on the amount of form information in the stimulus and were not driven by local motion signals. The sequential position stimulus, which contains form but lacks motion information, activates these areas more strongly than a stimulus that contains local image motion or a stimulus that is presented in a specific static posture (classic static). This suggests that these areas are recruited for biological motion perception, particularly in the absence of local motion signals.

## REFERENCES


1. Johansson G. Visual perception of biological motion and a model for its analysis. *Percept Psychophys* 1973; **14**:201–211.
2. Grossman E, Blake R. Brain areas active during visual perception of biological motion. *Neuron* 2002; **35**:1167–1175.
3. Grossman E, Donelly M, Price R, Pickens D, Morgan V, Neighbor G *et al.* Brain areas involved in perception of biological motion. *J Cogn Neurosci* 2000; **12**:711–720.
4. Vaina LM, Solomon J, Chowdhury S, Sinha P, Belliveau JW. Functional neuroanatomy of biological motion perception in humans. *Proc Natl Acad Sci USA* 2001; **98**:11656–11661.
5. Bonda E, Petrides M, Ostry D, Evans A. Specific involvement of human parietal system in the perception of biological motion. *J Neurosci* 1996; **16**:3737–3744.
6. Saygin AP, Wilson SM, Hagler DJ Jr, Bates E, Serono MI. Point-light biological motion perception activates human premotor cortex. *J Neurosci* 2004; **24**:6181–6188.
7. Beauchamp MS, Lee KE, Haxby JV, Martin A. fMRI responses to video and point-light displays of moving humans and manipulable objects. *J Cogn Neurosci* 2003; **15**:991–1001.
8. Vaina LM, Lemay M, Bienfang DC, Choi AY, Nakayama K. Intact biological motion and structure from motion perception in a patient with impaired motion mechanisms: a case study. *Vis Neurosci* 1990; **5**:353–369.
9. McLeod P, Dittrich W, Driver J, Perrett D, Zihl J. Preserved and impaired detection of structure from motion by a 'motion-blind' patient. *Vis cogn* 1996; **3**:363–391.
10. Schenk T, Zihl J. Visual motion perception after brain damage: I. Deficits in global motion perception. *Neuropsychologica* 1997; **35**:1289–1297.
11. Schenk T, Ziehl J. Visual motion perception after brain damage: II. Deficits in form-from-motion perception. *Neuropsychologica* 1997; **35**:1299–1310.
12. Beintema J, Lappe M. Perception of biological motion without local image motion. *Proc Natl Acad Sci USA* 2002; **99**:5661–5663.
13. Lange J, Lappe M. The role of form analysis in the perception of biological motion. *Soc Neurosci Abstr* 2004; http://sfn.scholarone.com; **34**.
14. Downing PE, Jiang Y, Shuman M, Kanwisher N. A cortical area selective for visual processing of the human body. *Science* 2001; **293**:2470–2473.
15. Cutting J. A program to generate synthetic walkers as dynamic point-light displays. *Behav Res Meth Instr* 1978; **10**:91–92.
16. Bertenthal BI, Pinto J. Global processing of biological motions. *Psychol Sci* 1997; **5**:221–225.
17. Vaina LM, Belliveau JW, Roziers BD, Zeffiro TA. Neural systems underlying learning and representation of global motion. *Proc Natl Acad Sci USA* 1998; **95**:12657–12662.
18. Talairach J, Tournoux P. *Co-planar stereotaxic atlas of the human brain*. New York: Thieme; 1988.
19. Schmahmann JD, Doyon J, McDonald D, Holmes C, Lavoie K, Hurwitz AS *et al.* Three-dimensional MRI atlas of the human cerebellum in proportional stereotaxic space. *Neuroimage* 1999; **10**:233–260.
20. Peelen MV, Downing PE. Selectivity for the human body in the fusiform gyrus. *J Neurophysiol* 2005; **93**:603–608.
21. Tootell RBH, Reppas JB, Kwong KK, Malach R, Born RT, Brady TJ *et al.* Functional analysis of human MT and related visual cortical areas using magnetic resonance imaging. *J Neurosci* 1995; **15**:3215–3230.
22. Oostende S, Sunaert S, van Hecke P, Marchal G, Orban GA. The kinetic occipital (KO) region in man: a fMRI study. *Cereb Cortex* 1997; **7**:690–701.
23. Murray SO, Olshausen BA, Woods DL. Processing shape, motion and three-dimensional shape-from-motion in the human cortex. *Cereb Cortex* 2003; **13**:508–516.
24. Liu T, Slotnick SC, Yantis S. Human MT+ mediates perceptual filling-in during apparent motion. *Neuroimage* 2004; **21**:1772–1780.
25. Stevens J, Fontlupt P, Shiffrar M, Detecy J. New aspects of motion perception: selective neural encoding of apparent human movements. *Neuroreport* 2000; **11**:109–115.
26. Gallese V, Fadiga L, Fogassi L, Rizzolatti G. Action recognition in the premotor cortex. *Brain* 1996; **119**:593–609.